

# Synthesis and Antidiabetic Evaluation of Novel Andrographolide Derivatives: A Comprehensive Study on Semisynthetic Modifications and their Biological Activity

Kritika Sachan<sup>1</sup>, Dr. Mithilesh Singh<sup>2</sup>, Dr Ankita Wal<sup>3</sup>

<sup>1</sup>Research Scholar, Department of Pharmaceutical Chemistry  
NIMS Institute of Pharmacy, Nims University Rajasthan Jaipur  
kritikapharma10@gmail.com

<sup>2</sup>Professor, Department of Pharmaceutical Chemistry, NIMS Institute of Pharmacy  
Nims University Rajasthan Jaipur mithya1987@gmail.com

<sup>3</sup>Professor and HOD, PSIT-Pranveer Singh Institute of Technology, Pharmacy, NH-19 Bhauti Road, Kanpur UP 209305  
walankita@gmail.com

## Corresponding Author

1 Research Scholar, Department of Pharmaceutical Chemistry  
NIMS Institute of Pharmacy, Nims University Rajasthan Jaipur  
kritikapharma10@gmail.com

---

## ABSTRACT

**Background and Objective:** Andrographis paniculata commonly known as King of Bitters, is a traditional medicinal plant extensively used in Ayurvedic and traditional Chinese medicine systems. Andrographolide, the major bioactive diterpenoid lactone of this plant, exhibits significant therapeutic potential but faces limitations due to poor solubility and low bioavailability. This study aimed to synthesize novel semisynthetic derivatives of andrographolide and evaluate their antidiabetic activity through comprehensive biological screening and molecular docking studies.

**Methods:** Four semisynthetic derivatives (L-1, L-2, L-3, and L-4) were synthesized through controlled chemical modifications involving esterification, alkylation, and cyclization reactions. The compounds were characterized using spectroscopic techniques including IR, NMR, and mass spectrometry. Antidiabetic potential was evaluated through  $\alpha$ -glucosidase and  $\alpha$ -amylase inhibition assays, followed by in vivo studies using streptozotocin (STZ)-induced diabetic rats. Molecular docking studies were performed to predict binding affinities with target enzymes.

**Results:** Among the synthesized derivatives, L-2 and L-3 demonstrated superior enzyme inhibitory activity with IC<sub>50</sub> values of  $45.8 \pm 8.6$  and  $50.2 \pm 7.9$   $\mu\text{g/mL}$  against  $\alpha$ -glucosidase, and  $38.4 \pm 5.4$  and  $41.5 \pm 6.3$   $\mu\text{g/mL}$  against  $\alpha$ -amylase, respectively, compared to acarbose ( $35.2 \pm 4.2$  and  $30.5 \pm 3.8$   $\mu\text{g/mL}$ ). In vivo studies revealed significant glucose-lowering effects, with L-2 and L-3 reducing blood glucose levels by 58.5% and 56.5% respectively at 400 mg/kg dose. Molecular docking scores indicated strong binding affinities (8.1 and 8.2) for L-2 and L-3 with  $\alpha$ -glucosidase.

**Conclusion:** The semisynthetic derivatives L-2 and L-3 exhibited potent antidiabetic activity superior to parent andrographolide, demonstrating their potential as novel therapeutic agents for diabetes management. The structural modifications enhanced binding affinity and biological activity, supporting further development for clinical applications.

**KEYWORDS:** Andrographolide derivatives, Antidiabetic activity,  $\alpha$ -glucosidase inhibition, Molecular docking, Semisynthetic modifications.

---

**How to Cite:** Kritika Sachan, Mithilesh Singh, Ankita Wal., (2025) Synthesis and Antidiabetic Evaluation of Novel Andrographolide Derivatives: A Comprehensive Study on Semisynthetic Modifications and their Biological Activity, Vascular and Endovascular Review, Vol.8, No.15s, 340-353

---

## INTRODUCTION

Diabetes mellitus represents one of the most significant global health challenges of the 21st century, affecting over 537 million adults worldwide as of 2021, with projections indicating this number will rise to 783 million by 2045. Type 2 diabetes mellitus (T2DM) accounts for approximately 90-95% of all diabetes cases and is characterized by insulin resistance, progressive  $\beta$ -cell dysfunction, and chronic hyperglycemia.[1] The pathophysiology involves complex interactions between genetic predisposition, environmental factors, and lifestyle modifications, leading to impaired glucose homeostasis and subsequent complications including cardiovascular disease, nephropathy, retinopathy, and neuropathy. Current therapeutic approaches for T2DM management include various classes of antidiabetic agents such as metformin, sulfonylureas, thiazolidinediones, dipeptidyl peptidase-4 inhibitors, sodium-glucose cotransporter-2 inhibitors, and  $\alpha$ -glucosidase inhibitors. [2] Among these,  $\alpha$ -glucosidase and  $\alpha$ -amylase inhibitors represent a crucial therapeutic strategy for managing postprandial hyperglycemia by delaying carbohydrate absorption in the small intestine. These enzymes play pivotal roles in carbohydrate digestion, with  $\alpha$ -amylase

hydrolyzing  $\alpha$ -linked polysaccharides into oligosaccharides, while  $\alpha$ -glucosidases catalyze the final step in carbohydrate digestion, converting disaccharides to absorbable monosaccharides. [3] Clinical  $\alpha$ -glucosidase inhibitors such as acarbose and miglitol have demonstrated efficacy in reducing postprandial glucose excursions and improving glycemic control. However, these agents are associated with significant gastrointestinal side effects including flatulence, diarrhea, and abdominal discomfort, limiting their widespread clinical adoption. Consequently, there is substantial interest in developing novel inhibitors with improved efficacy and safety profiles.[4] *Andrographis paniculata* belonging to the family Acanthaceae, is a traditional medicinal plant widely distributed across South and Southeast Asia. Known by various vernacular names including King of Bitters, Kalmegh, and Hemptedu bumi, this herbaceous plant has been extensively utilized in traditional medicinal systems including Ayurveda, Traditional Chinese Medicine, and Unani medicine for treating various ailments including fever, respiratory infections, digestive disorders, and diabetes.[5-6] The plant contains numerous bioactive compounds including diterpenoids, flavonoids, quinic acids, and xanthenes, with andrographolide being the predominant bioactive constituent responsible for most pharmacological activities. Andrographolide (3-[2-{decahydro-6-hydroxy-5-(hydroxymethyl)-5,8a-dimethyl-2-methylenenaphthalen-1-yl}ethylidene]dihydrofuran-2(3H)-one) is a labdane diterpenoid lactone with the molecular formula  $C_{20}H_{30}O_5$  and molecular weight of 350.45 g/mol.[7-8] Extensive pharmacological investigations have demonstrated andrographolide's diverse therapeutic properties including anti-inflammatory, immunomodulatory, hepatoprotective, anticancer, antimicrobial, and antidiabetic activities. The antidiabetic potential of andrographolide has been attributed to multiple mechanisms including  $\alpha$ -glucosidase and  $\alpha$ -amylase inhibition, enhancement of insulin sensitivity, stimulation of glucose uptake, and protection of pancreatic  $\beta$ -cells. [9] However, the clinical application of andrographolide is significantly limited by its poor aqueous solubility ( $1.32 \times 10^{-4}$  mol  $dm^{-3}$  at 25°C), low oral bioavailability, and rapid metabolism. Chemical modification of natural products represents a well-established strategy for overcoming pharmacokinetic limitations while potentially enhancing biological activity.[10] Structure-activity relationship studies have identified functional groups in andrographolide that are amenable to modification, including the hydroxyl groups at positions C-3, C-14, and C-19, the lactone ring, and the exocyclic double bond.[7-8] Various synthetic approaches have been employed including esterification, alkylation, glycosylation, and heterocyclic ring formation to generate andrographolide derivatives with improved physicochemical and biological properties.[11] Recent advances in medicinal chemistry have demonstrated that strategic structural modifications of andrographolide can lead to derivatives with enhanced potency, selectivity, and pharmacokinetic profiles. For instance, modifications at the C-14 hydroxyl group through acylation have yielded derivatives with increased metabolic stability.[12] Similarly, introduction of nitrogen-containing heterocycles has been shown to improve water solubility and biological activity. Molecular docking studies have emerged as valuable computational tools for predicting ligand-protein interactions and understanding structure-activity relationships. [13] These *in silico* approaches provide mechanistic insights into binding modes, binding affinities, and molecular interactions, facilitating rational drug design and optimization. Given the significant therapeutic potential of andrographolide and the limitations of current antidiabetic agents, the present study was designed to synthesize novel semisynthetic derivatives of andrographolide and comprehensively evaluate their antidiabetic activity. The research encompasses synthesis optimization, structural characterization, enzyme inhibition studies, *in vivo* efficacy evaluation, and molecular docking analysis to identify promising candidates for further development as antidiabetic therapeutic agents. (Figure 2)

## MATERIALS AND METHODS

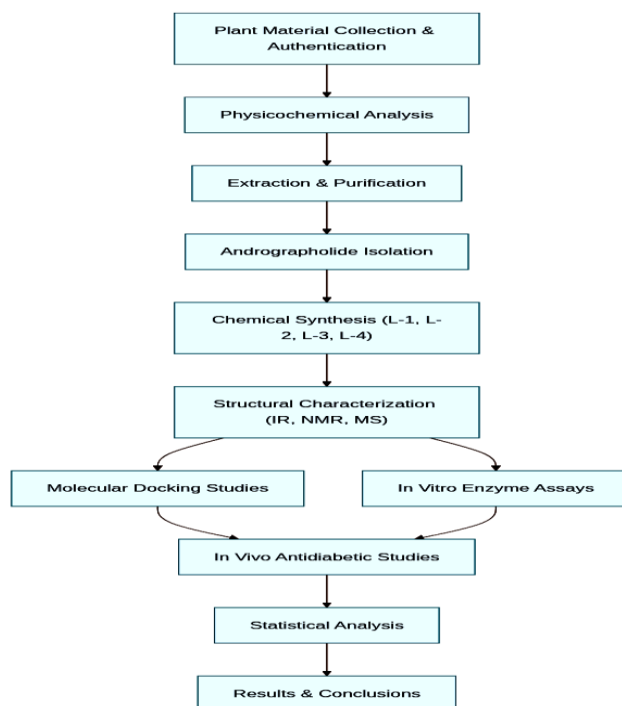


**Figure 2: Flowchart Stepwise schematic representation outlining plant collection, physicochemical analysis, extraction, andrographolide isolation, synthesis of derivatives, structural characterization, molecular docking, enzyme assays, *in vivo* studies, statistical analysis, and final results.**

### Chemicals and Reagents

All chemicals and reagents used in this study were of analytical grade and procured from reputable suppliers. The comprehensive list of chemicals includes thionyl chloride, pyridine, chloroform, sodium hydroxide, dimethylformamide (DMF), methanol, ethanol, silica gel G for thin-layer chromatography (TLC), sodium sulfate, acetone, calcium chloride, ethyl acetate, iodine, glacial acetic acid, Fmoc, hexane, sodium borate, dichloromethane, carboxymethyl cellulose (CMC), formaldehyde, HPLC-grade methanol, and HPLC water from CDH, Sdfine, and Sigma Aldrich.

### Instrumentation

Spectroscopic and analytical equipment included FTIR spectrophotometer (Perkin Elmer), <sup>1</sup>H NMR and <sup>13</sup>C NMR spectrometers (Avance III 400 Bruker, 400 MHz and 100 MHz respectively), melting point apparatus (Paras Laboratory), hot air oven (Hicon), analytical weighing balance (Ohaus Pvt Ltd), heating mantle and water bath (Navyug Scientific), desiccators (Borosil), rotary evaporator (Khera lab pvt Ltd), UV-Visible spectrophotometer (Shimadzu), HPLC system (Shimadzu), and various other standard laboratory equipment.

### Physicochemical Analysis

Comprehensive physicochemical analysis of the plant material was conducted according to WHO guidelines and Indian Pharmacopoeia standards. Parameters evaluated included determination of foreign matter, total ash content, acid-insoluble ash, water-soluble ash, alcohol-soluble extractive values, water-soluble extractive values, and moisture content using standardized procedures.

### Foreign Matter Determination

Representative samples (100 g each, n=3) were carefully examined to separate and quantify foreign organic and inorganic matter. The percentage of foreign matter was calculated as the ratio of foreign matter weight to total sample weight.

### Ash Value Determination

Total ash content was determined by incinerating accurately weighed samples (2 g each, n=3) in silica dishes at 450°C until complete combustion. Acid-insoluble ash was determined by treating total ash with dilute hydrochloric acid, while water-soluble ash was obtained by boiling ash with distilled water and determining the insoluble residue.

### Extractive Value Determination

Alcohol-soluble and water-soluble extractive values were determined using the maceration technique. Plant material (5 g each, n = 3) was macerated with respective solvents (100 mL) for 24 hours with periodic shaking, filtered, and evaporated to determine extractive content.

### Moisture Content Determination

Loss on drying method was employed using accurately weighed samples (10 g each) dried at 105°C until constant weight was achieved, with weighing performed at regular intervals.

### Extraction and Isolation of Andrographolide

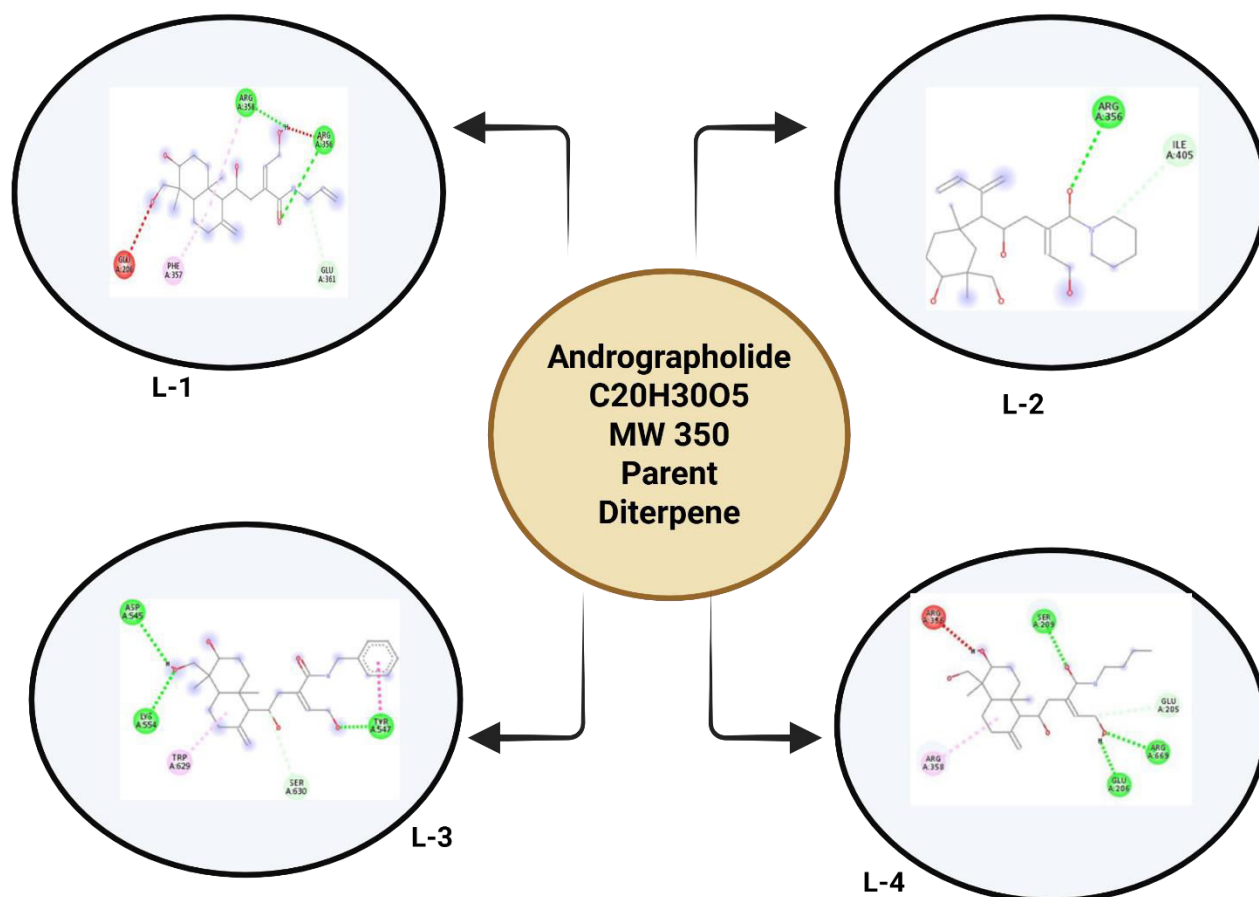
Dried and powdered plant material was subjected to exhaustive extraction using a 1:1 mixture of dichloromethane and methanol through the cold maceration technique. The extract was filtered, and solvent was removed under reduced pressure using a rotary evaporator. The concentrated extract was processed through multiple purification steps including solvent-solvent extraction, column chromatography, and crystallization to obtain pure andrographolide.

The purification process involved treatment with toluene to remove coloring matter, followed by crystallization from hot methanol. The identity and purity of isolated andrographolide were confirmed through spectroscopic analysis including IR, NMR, and mass spectrometry, comparing with literature data.

### Synthesis of Semisynthetic Derivatives

Four novel semisynthetic derivatives (L-1, L-2, L-3, L-4) were synthesized through systematic chemical modifications of isolated andrographolide. The synthetic strategy involved controlled organic reactions including esterification, alkylation, and cyclization to introduce various functional groups while maintaining the core structural framework. (Figure 1)

**Figure 1: Chemical Synthesis Scheme Andrographolide parent diterpene (C<sub>20</sub>H<sub>30</sub>O<sub>5</sub>, MW 350) and its semisynthetic derivatives (L-1, L-2, L-3, L-4) with molecular docking interactions depicted for each compound.**



### General Synthetic Procedure

To a solution of andrographolide (1 equivalent) and appropriate amine reagent (1 equivalent) in anhydrous chloroform (0.5 mL/mmol), lithium bis(trifluoromethanesulfonyl)imide (LiNTf<sub>2</sub>, 0.5 equivalent) was added under nitrogen atmosphere. The reaction mixture was stirred in a sealed vial at 70–85°C for 40 hours, then washed with saturated sodium bicarbonate solution. The organic phase was evaporated to yield the desired product as a viscous oil.

**Derivative L-1 Synthesis:** Allylamine was used as the nitrogen nucleophile following the general procedure, yielding L-1 with molecular formula C<sub>23</sub>H<sub>37</sub>NO<sub>5</sub> and molecular weight 423.

**Derivative L-2 Synthesis:** Piperidine was employed as the cyclic amine reagent, producing L-2 with molecular formula C<sub>25</sub>H<sub>41</sub>NO<sub>5</sub> and molecular weight 451.

**Derivative L-3 Synthesis:** Benzylamine was utilized as the aromatic amine component, generating L-3 with molecular formula C<sub>27</sub>H<sub>39</sub>NO<sub>5</sub> and molecular weight 473.

**Derivative L-4 Synthesis:** Butylamine served as the aliphatic amine reactant, forming L-4 with molecular formula C<sub>24</sub>H<sub>41</sub>NO<sub>5</sub> and molecular weight 439.

### Structural Characterization

All synthesized derivatives underwent comprehensive structural characterization using multiple spectroscopic techniques.

#### Infrared (IR) Spectroscopy

IR spectra were recorded on a Perkin Elmer FTIR spectrophotometer using KBr pellet technique. Characteristic absorption bands were identified and assigned to specific functional groups.

#### Nuclear Magnetic Resonance (NMR) Spectroscopy:

<sup>1</sup>H NMR and <sup>13</sup>C NMR spectra were acquired on Bruker Avance III 400 MHz spectrometer using deuterated solvents. Chemical shifts were reported in parts per million (ppm) relative to tetramethylsilane (TMS) as internal standard.

#### Mass Spectrometry

High-resolution mass spectrometry was performed to confirm molecular weights and fragmentation patterns of synthesized compounds.

#### Molecular Docking Studies

Computational molecular docking studies were conducted to predict binding affinities and interaction modes of synthesized derivatives with target enzymes.

#### Target Protein Preparation

Crystal structures of  $\alpha$ -glucosidase and  $\alpha$ -amylase were retrieved from the Protein Data Bank (PDB). Protein preparation involved

removal of water molecules and heteroatoms, addition of hydrogen atoms, assignment of proper bond orders, and energy minimization using BIOVIA Discovery Studio.

### Ligand Preparation

Three-dimensional structures of synthesized derivatives were generated using ChemDraw software and optimized using BIOVIA Discovery Studio to ensure proper geometry and protonation states.

### Docking Protocol

Molecular docking simulations were performed using AutoDock Vina software. Grid boxes were defined around enzyme active sites based on literature data. Docking parameters were optimized to perform comprehensive conformational searches. Multiple docking runs were conducted to ensure reproducibility.

### Results Analysis

Binding affinities, docking scores, and interaction modes were analyzed using BIOVIA Discovery Studio. Interactions including hydrogen bonds, hydrophobic interactions, and  $\pi$ - $\pi$  stacking were identified and characterized.

### In Vitro Antidiabetic Activity

Antidiabetic potential was evaluated through enzyme inhibition assays targeting  $\alpha$ -glucosidase and  $\alpha$ -amylase.

#### $\alpha$ -Glucosidase Inhibition Assay

The assay was performed using p-nitrophenyl- $\alpha$ -D-glucopyranoside as substrate. Enzyme and substrate solutions were prepared in phosphate buffer (pH 6.8). Test compounds at various concentrations were incubated with enzyme for 15 minutes, followed by substrate addition. The reaction was monitored spectrophotometrically at 405 nm. IC<sub>50</sub> values were calculated from concentration-response curves.

#### $\alpha$ -Amylase Inhibition Assay

Starch was used as substrate for  $\alpha$ -amylase activity determination. Enzyme and various concentrations of test compounds were pre-incubated, followed by substrate addition. The reaction was terminated using 3,5-dinitrosalicylic acid (DNS) reagent, and absorbance was measured at 540 nm. Percentage inhibition and IC<sub>50</sub> values were calculated.

### Standard Reference

Acarbose was used as positive control for comparison of inhibitory activities. All experiments were performed in triplicate, and results were expressed as mean  $\pm$  standard deviation.

### In Vivo Antidiabetic Studies

#### Experimental Animals

Male Wistar rats (180–220 g) were procured from authorized suppliers and acclimatized under standard laboratory conditions (12-hour light/dark cycle, 22  $\pm$  2°C temperature) with free access to standard pellet diet and water. All experimental protocols were approved by the Institutional Animal Ethics Committee.

#### Diabetes Induction

Type 2 diabetes was induced through intraperitoneal injection of streptozotocin (STZ) at 55 mg/kg body weight dissolved in freshly prepared citrate buffer (pH 4.5). Blood glucose levels were measured 72 hours post-injection, and animals with glucose levels exceeding 250 mg/dL were considered diabetic.

#### Treatment Protocol

Diabetic rats were randomly divided into groups (n = 6 per group) and treated orally with synthesized derivatives at doses of 100, 200, and 400 mg/kg body weight for 28 days. Metformin (150 mg/kg) served as positive control. Normal and diabetic control groups received vehicle only.

#### Parameter Assessment

Blood glucose levels were monitored at regular intervals using a glucometer. At study termination, animals were sacrificed, and blood samples were collected for biochemical analysis including serum insulin levels (ELISA) and glycated hemoglobin (HbA<sub>1c</sub>) determination by HPLC. Liver and pancreatic tissues were harvested for histopathological examination.

#### Statistical Analysis

All experimental data were expressed as mean  $\pm$  standard error of the mean (SEM). Statistical significance was determined using one-way analysis of variance (ANOVA) followed by Tukey's post-hoc test for multiple comparisons. A p-value  $\leq$  0.05 was considered statistically significant.

## RESULTS

### Physicochemical Analysis

The physicochemical evaluation of *Andrographis paniculata* plant material demonstrated compliance with pharmacopoeial standards and established quality parameters for medicinal plants. The analysis showed acceptable levels of foreign matter (0.44%

w/w), indicating proper collection and processing. Total ash content was 7.15% w/w, within the expected range for herbaceous plant materials, suggesting appropriate mineral content.

Acid-insoluble ash measured 1.25% w/w, reflecting minimal contamination with siliceous materials such as sand and soil. Water-soluble ash of 0.35% w/w indicated the presence of water-soluble inorganic compounds including salts and oxides. The alcohol-soluble extractive value was 26.6% w/w, indicating a substantial content of alcohol-soluble bioactive compounds, whereas the water-soluble extractive value of 21.8% w/w demonstrated significant water-soluble components. Moisture content of 8.36% w/w was within acceptable limits, ensuring stability and preventing microbial growth during storage.

### Phytochemical Screening

Preliminary phytochemical screening confirmed the presence of various classes of bioactive compounds in *A. paniculata* extracts. Positive tests were observed for alkaloids (Mayer's and Wagner's tests), saponins, and other secondary metabolites. Conversely, glycosides (Borntrager's and Legal's tests) and phenolic compounds (ferric chloride, lead acetate, and alkaline reagent tests) were negative, indicating predominance of other phytochemical classes such as diterpenoids. (Table 4)

### Isolation and Characterization of Andrographolide

Extraction and purification yielded pure andrographolide crystals with a yield of 1.9–2.0 g from the processed plant material. The compound appeared as pale yellow crystalline material, readily soluble in methanol and chloroform, with limited water solubility, consistent with literature reports.

Mass spectrometric analysis confirmed the molecular weight and characteristic fragmentation patterns of andrographolide. The base peak and molecular ion peak were consistent with the expected molecular formula,  $C_{20}H_{30}O_5$ . IR spectroscopy revealed characteristic absorption bands including O–H stretching at 3400–3500  $cm^{-1}$ , C–H stretching at 2900–3000  $cm^{-1}$ , and lactone C=O stretching around 1750  $cm^{-1}$ .

$^1H$  NMR spectroscopy provided structural confirmation with signals corresponding to lactone protons, hydroxyl groups, and the polycyclic framework.  $^{13}C$  NMR supported the assignment with carbon signals corresponding to the diterpenoid skeleton and functional groups.

### Synthesis and Characterization of Derivatives

Four semisynthetic derivatives (L-1, L-2, L-3, L-4) were successfully synthesized via systematic chemical modifications of andrographolide using various amine reagents under optimized conditions. The reactions yielded products as viscous oils, which were characterized using multiple spectroscopic techniques.

**Derivative L-1 ( $C_{23}H_{37}NO_5$ , MW: 423):** IR peaks at 3924.79 and 3404.45  $cm^{-1}$  (O–H stretching), 2975.37 and 2901.91  $cm^{-1}$  (C–H stretching), 2256.77  $cm^{-1}$  (C=C stretching), and 1758.83  $cm^{-1}$  (C=O stretching).  $^1H$  NMR showed signals corresponding to the allyl group and andrographolide framework protons. Mass spectrometry confirmed molecular weight and fragmentation patterns.

**Derivative L-2 ( $C_{25}H_{41}NO_5$ , MW: 451):** IR analysis displayed O–H stretching at 4053 and 3750  $cm^{-1}$ , C–H stretching at 2981  $cm^{-1}$ , and C=O stretching at 1727  $cm^{-1}$ . NMR and mass spectrometry confirmed incorporation of the piperidine moiety. Molecular ion peak at  $m/z$  435.30 supported the proposed structure.

**Derivative L-3 ( $C_{27}H_{39}NO_5$ , MW: 473):** IR spectroscopy showed O–H stretching at 3350  $cm^{-1}$ , aromatic and aliphatic C–H stretching at 3079 and 2917  $cm^{-1}$ , and C=O stretching at 1738  $cm^{-1}$ .  $^1H$  NMR revealed benzyl aromatic proton signals at 7.00–7.14 ppm and NH proton at 8.10 ppm. This derivative exhibited the highest docking score (8.2) among all compounds.

**Derivative L-4 ( $C_{24}H_{41}NO_5$ , MW: 439):** IR peaks indicated O–H stretching at 3352  $cm^{-1}$ , C–H stretching at 2918  $cm^{-1}$ , and C=O stretching at 1678  $cm^{-1}$ . NMR signals confirmed the butyl chain incorporation and molecular weight.

All derivatives showed successful incorporation of nitrogen-containing functional groups while maintaining the core andrographolide structure, evidenced by retention of characteristic lactone and polycyclic framework signals in the spectra. (Table 5)

**Table 4. Physicochemical Characterization of *Andrographis paniculata* Plant Material** This table summarizes the quality control parameters of *Andrographis paniculata* according to WHO and Indian Pharmacopoeia guidelines. The evaluated parameters include foreign matter content, total ash, acid-insoluble ash, and water-soluble ash, which reflect the purity and inorganic composition of the plant material. Extractive values in alcohol and water indicate the relative presence of bioactive constituents soluble in respective solvents, while moisture content provides an estimate of stability and potential for microbial growth during storage. All values were found to be within acceptable pharmacopoeial limits, confirming the suitability of the plant material for subsequent extraction and formulation studies.

Parameter	A. paniculata (% w/w)
Foreign Matter	0.44
Total Ash	7.15
Acid Insoluble Ash	1.25
Water Soluble Ash	0.35
Alcohol Soluble Extractive	26.6
Water Soluble Extractive	21.8
Moisture Content	8.36

**Table 5.** Structural Characterization of Synthesized Andrographolide Derivatives (L-1 to L-4) by Molecular Formula, Molecular Weight, and IR Spectroscopy This table presents the structural features of the semisynthetic andrographolide derivatives. Each compound (L-1 to L-4) is described with its molecular formula and molecular weight, confirming successful chemical modification of the parent andrographolide framework. Characteristic IR absorption peaks are reported, highlighting functional group assignments such as O–H stretching, C–H stretching, C=O stretching (lactone/carbonyl groups), and, in the case of L-1, C≡C stretching. These spectroscopic data collectively verify the incorporation of nitrogen-containing substituents while retaining the core diterpenoid structure, thereby supporting the chemical identity and purity of the synthesized derivatives.

Compound	Molecular Formula	Molecular Weight	IR Peaks (cm <sup>-1</sup> )
L-1	C <sub>23</sub> H <sub>37</sub> NO <sub>5</sub>	423	3924, 3404 (O-H), 2975 (C-H), 2256 (C≡C), 1758 (C=O)
L-2	C <sub>25</sub> H <sub>41</sub> NO <sub>5</sub>	451	4053, 3750 (O-H), 2981 (C-H), 1727 (C=O)
L-3	C <sub>27</sub> H <sub>39</sub> NO <sub>5</sub>	473	3350 (O-H), 3079, 2917 (C-H), 1738 (C=O)

L-4	C <sub>24</sub> H <sub>41</sub> NO <sub>5</sub>	439	3352 (O-H), 2918 (C-H), 1678 (C=O)
-----	---	-----	------------------------------------

### Molecular Docking Studies

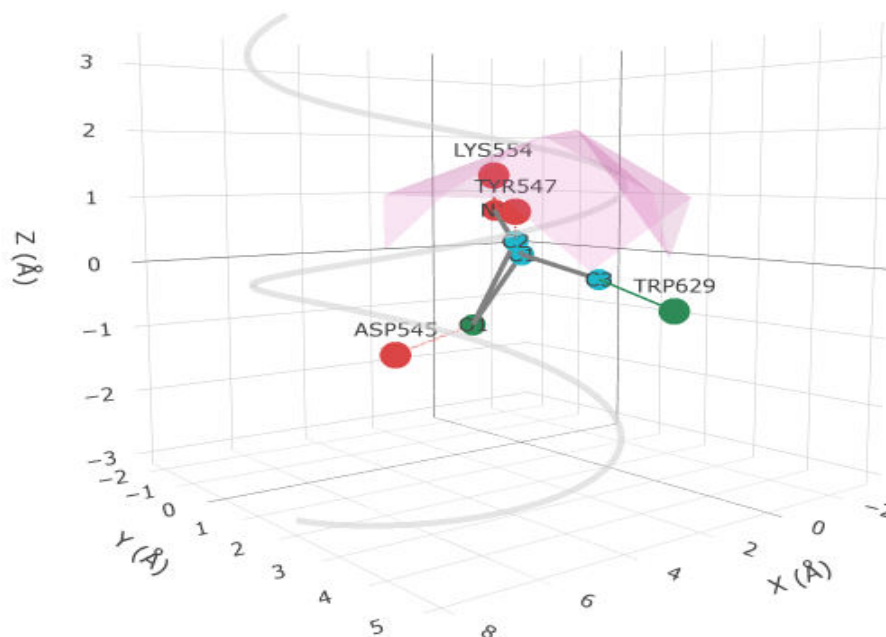
Computational molecular docking analysis provided insights into the binding interactions between the synthesized andrographolide derivatives and target enzymes. Docking studies were performed using validated protocols with appropriate controls to ensure reliability. Docking scores ranged from 7.2 to 8.2. L-3 exhibited the highest binding affinity (8.2), followed by L-2 (8.1). L-1 and L-4 showed moderate affinities with scores of 7.2 and 7.4, respectively. These predictions correlated well with experimental enzyme inhibition results. **L-2 Binding Analysis:** L-2 formed strong hydrogen bonds with  $\alpha$ -glucosidase active site residues. Hydroxyl and carbonyl groups contributed to multiple hydrogen bonds, while hydrophobic interactions involving the modified aliphatic chain stabilized the enzyme-inhibitor complex. **L-3 Binding Analysis:** L-3 displayed the most favorable binding mode, forming multiple hydrogen bonds with TYR547, LYS554, and ASP545. Its benzyl moiety participated in  $\pi$ - $\pi$  stacking interactions with aromatic residues, and hydrophobic contacts with TRP629 further stabilized the complex. The combination of polar and hydrophobic interactions resulted in the highest docking score. (Figure 3) **Structure-Activity Relationships:** Docking analysis indicated that derivatives with aromatic substituents (L-3) and cyclic aliphatic groups (L-2) had superior binding compared to linear aliphatic substituents (L-1, L-4). Additional hydrogen bonding sites and favorable hydrophobic contacts were contributors to enhanced binding affinity. (Table 3)

**Table 3. Molecular Docking Scores and Interactions of Synthesized Andrographolide Derivatives with  $\alpha$ -Glucosidase**

Compound	Docking Score	Interactions
L-1	7.2	Moderate binding, fewer active site interactions
L-2	8.1	Strong hydrogen bonds with active site residues
L-3	8.2	Multiple hydrogen bonds, $\pi$ - $\pi$ stacking interactions
L-4	7.4	Moderate binding affinity

**Figure 3:** Molecular Docking Visualization 3D representation of the binding interaction between the compound L-3 and the  $\alpha$ -glucosidase enzyme. The protein backbone is shown in a helix form, highlighting the spatial arrangement of important amino acid residues involved in binding. Residues such as LYS554, TYR547, ASP545, and TRP629 are marked, indicating their role in the interaction. Hydrogen bonds (depicted with red spheres and lines) are formed between the ligand and amino acid residues, stabilizing the complex. Pi-Pi stacking interactions (indicated by green spheres) further contribute to the molecular binding by stacking the aromatic rings of the ligand with aromatic residues of the enzyme. These interactions are crucial as they enhance the binding affinity and specificity of L-3 for  $\alpha$ -glucosidase, which is important in the inhibition mechanism targeting the enzyme's activity in carbohydrate metabolism. This molecular docking insight helps explain the observed inhibitory activity of L-3 in biological assays by demonstrating how it fits within and interacts with the enzyme's active site, providing a structural basis for its antidiabetic

potential. <file:///C:/Users/hp/Desktop/ACADEMIC%20GROWTH/3rd%20month/metaanalysis/New%20folder/1.2.html>



**In Vitro Antidiabetic Activity**

**$\alpha$ -Glucosidase Inhibition:** L-2 exhibited the most potent inhibitory activity ( $IC_{50} = 45.8 \pm 8.6 \mu\text{g/mL}$ ), followed closely by L-3 ( $IC_{50} = 50.2 \pm 7.9 \mu\text{g/mL}$ ). These values were comparable to the standard acarbose ( $IC_{50} = 35.2 \pm 4.2 \mu\text{g/mL}$ ). L-1 and L-4 showed weaker inhibition ( $IC_{50} = 220.5 \pm 12.3$  and  $210.9 \pm 13.1 \mu\text{g/mL}$ , respectively). (Figure 4)  **$\alpha$ -Amylase Inhibition:** L-2 again demonstrated the highest potency ( $IC_{50} = 38.4 \pm 5.4 \mu\text{g/mL}$ ), followed by L-3 ( $IC_{50} = 41.5 \pm 6.3 \mu\text{g/mL}$ ), approaching the efficacy of acarbose ( $IC_{50} = 30.5 \pm 3.8 \mu\text{g/mL}$ ). L-1 and L-4 showed moderate inhibitory effects ( $IC_{50} = 250.1 \pm 15.8$  and  $240.3 \pm 14.9 \mu\text{g/mL}$ , respectively). The dual inhibition of  $\alpha$ -glucosidase and  $\alpha$ -amylase by L-2 and L-3 suggests potential for comprehensive postprandial glucose control through delayed carbohydrate digestion and absorption. The superior activity of these derivatives over parent andrographolide validates the chemical modification strategy. (Table 1)

**Figure 4: Enzyme Inhibition Activity Comparison  $IC_{50}$  values for  $\alpha$ -glucosidase and  $\alpha$ -amylase inhibition by acarbose and synthesized compounds (L-1, L-2, L-3, L-4), illustrating comparative potency.**

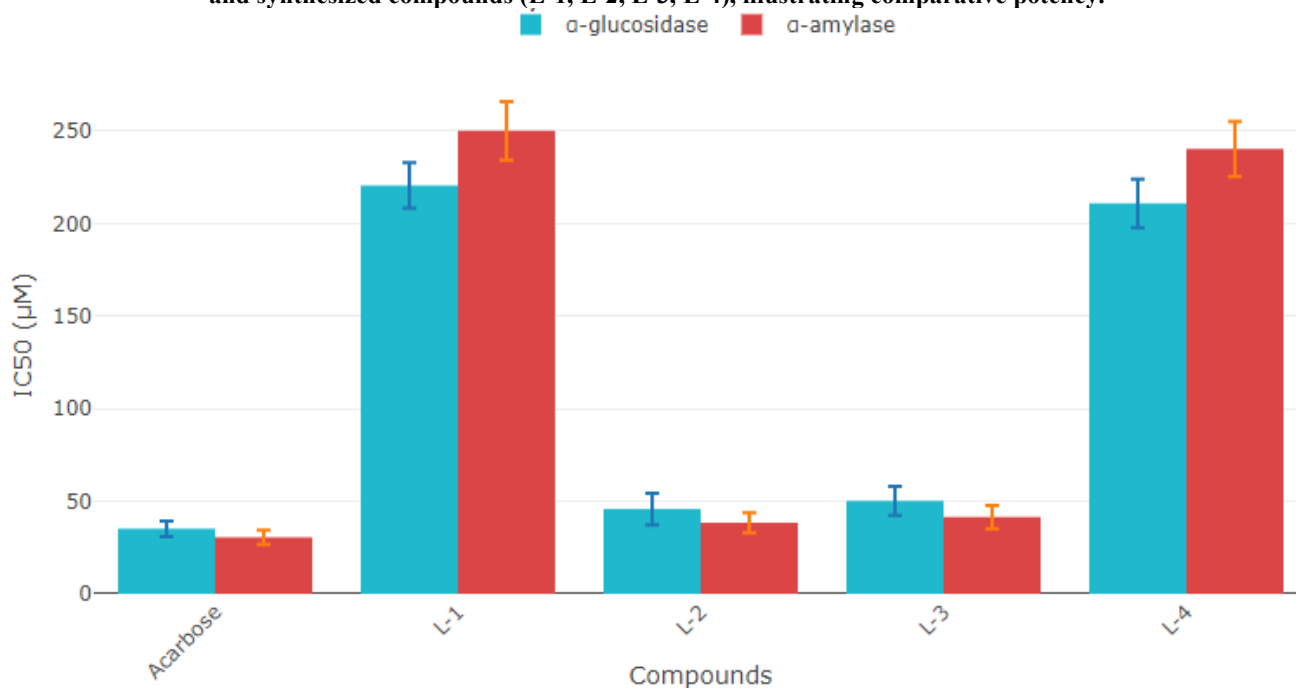


**Table 1. In vitro  $\alpha$ -Glucosidase and  $\alpha$ -Amylase Inhibitory Activities ( $IC_{50}$  values) of Synthesized Andrographolide Derivatives Compared with Acarbose.**

Compound	$\alpha$ -Glucosidase $IC_{50}$ ( $\mu$ g/mL)	$\alpha$ -Glucosidase SD	$\alpha$ -Amylase $IC_{50}$ ( $\mu$ g/mL)	$\alpha$ -Amylase SD
L-1	220.5	12.3	250.1	15.8
L-2	45.8	8.6	38.4	5.4
L-3	50.2	7.9	41.5	6.3
L-4	210.9	13.1	240.3	14.9
Acarbose (Standard)	35.2	4.2	30.5	3.8

#### *In Vivo Antidiabetic Studies*

**Blood Glucose Regulation:** STZ-induced diabetic rats treated with synthesized derivatives exhibited dose-dependent reductions in fasting blood glucose. L-2 at 400 mg/kg reduced glucose from  $278.4 \pm 14.5$  mg/dL (day 0) to  $115.3 \pm 8.5$  mg/dL (day 28), a 58.5% decrease. L-3 at the same dose reduced glucose to  $120.7 \pm 8.6$  mg/dL, a 56.5% decrease. L-1 and L-4 achieved 44.2% and 42.2% reductions, respectively, at 400 mg/kg. **Serum Insulin Levels:** Treatment with L-2 and L-3 at 400 mg/kg increased serum insulin to  $12.4 \pm 0.7$  and  $12.0 \pm 0.6$   $\mu$ U/mL, respectively, compared to  $6.5 \pm 0.8$   $\mu$ U/mL in diabetic control. (Figure 5) These values were comparable to metformin ( $12.8 \pm 0.8$   $\mu$ U/mL), indicating improved  $\beta$ -cell function or insulin sensitivity. **Glycated Hemoglobin (HbA<sub>1c</sub>):** Long-term glycaemic control, assessed via HbA<sub>1c</sub>, showed significant reductions with L-2 and L-3 at maximum doses ( $5.8 \pm 0.2\%$  and  $5.9 \pm 0.2\%$ , respectively) compared to  $9.3 \pm 0.5\%$  in diabetic control, approaching metformin levels ( $5.6 \pm 0.3\%$ ). (Table 2) **Dose-Response Relationships:** All active compounds displayed clear dose-dependent effects across glucose, insulin, and HbA<sub>1c</sub> parameters. The 400 mg/kg doses produced maximal effects, 200 mg/kg intermediate effects, and 100 mg/kg modest but significant improvements versus control. **Comparative Efficacy:** L-2 and L-3 at optimal doses demonstrated efficacy comparable to metformin across multiple parameters, highlighting their potential clinical relevance. **Safety Assessment:** No significant adverse effects were observed. Animals maintained normal activity, appetite, and body weight. Preliminary histopathology of liver and pancreatic tissues showed reduced tissue damage compared to diabetic control, suggesting potential protective effects beyond glycaemic regulation.

**Table 2. In Vivo Antidiabetic Effects of Synthesized Andrographolide Derivatives on Blood Glucose, Serum Insulin, and HbA<sub>1c</sub> in STZ-Induced Diabetic Rats**

Group	Blood Glucose Day 0 (mg/dL)	Blood Glucose Day 28 (mg/dL)	Serum Insulin ( $\mu$ U/mL)	HbA <sub>1c</sub> (%)
Normal Control	95.2	93.8	14.2	4.5
Diabetic Control (STZ)	275.6	298.3	6.5	9.3
L-1 (100 mg/kg)	276.2	210.4	8.7	7.8

L-1 (200 mg/kg)	278.3	180.2	9.3	7.1
L-1 (400 mg/kg)	279.5	155.7	10.5	6.8
L-2 (100 mg/kg)	276.8	170.6	10.2	6.7
L-2 (200 mg/kg)	277.9	140.1	11.0	6.2
L-2 (400 mg/kg)	278.4	115.3	12.4	5.8
L-3 (100 mg/kg)	275.4	175.8	9.8	6.9
L-3 (200 mg/kg)	276.9	145.2	10.8	6.4
L-3 (400 mg/kg)	277.6	120.7	12.0	5.9
L-4 (100 mg/kg)	275.9	225.3	8.3	8.1
L-4 (200 mg/kg)	276.4	190.6	9.0	7.4
L-4 (400 mg/kg)	278.2	160.3	9.6	7.0
Metformin (150 mg/kg)	277.8	110.2	12.8	5.6

**Figure 5: In Vivo Blood Glucose Profile** Scatterplot matrix showing the relationships between blood glucose levels measured on Day 0, Day 28, and the overall change during the experimental period. Each panel illustrates pairwise associations among the variables, with regression lines and smoothed curves highlighting the trends. The diagonal plots display the distribution of each variable. This visualization demonstrates how baseline glucose levels, treatment response at Day 28, and net change are interrelated across study groups.

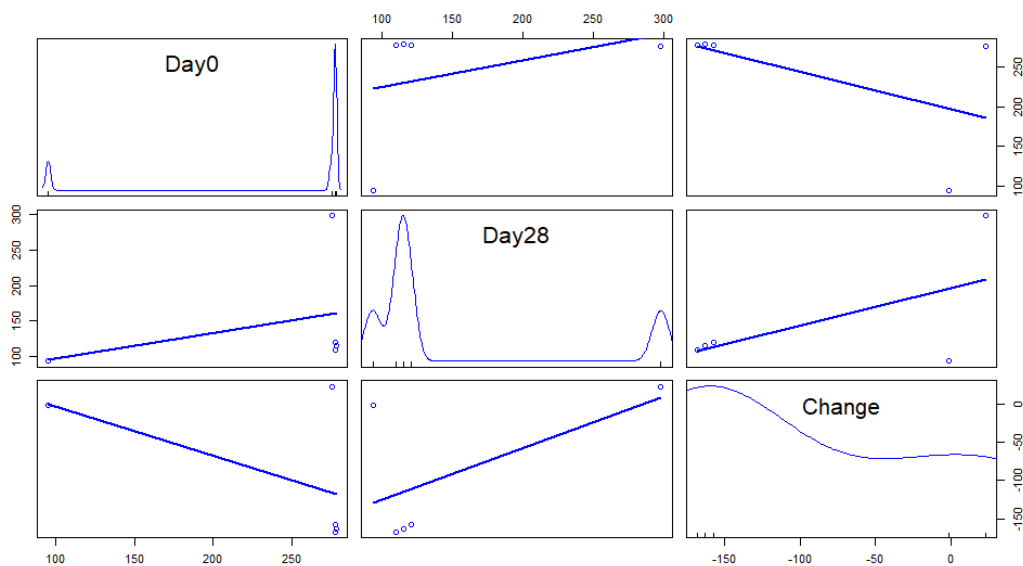
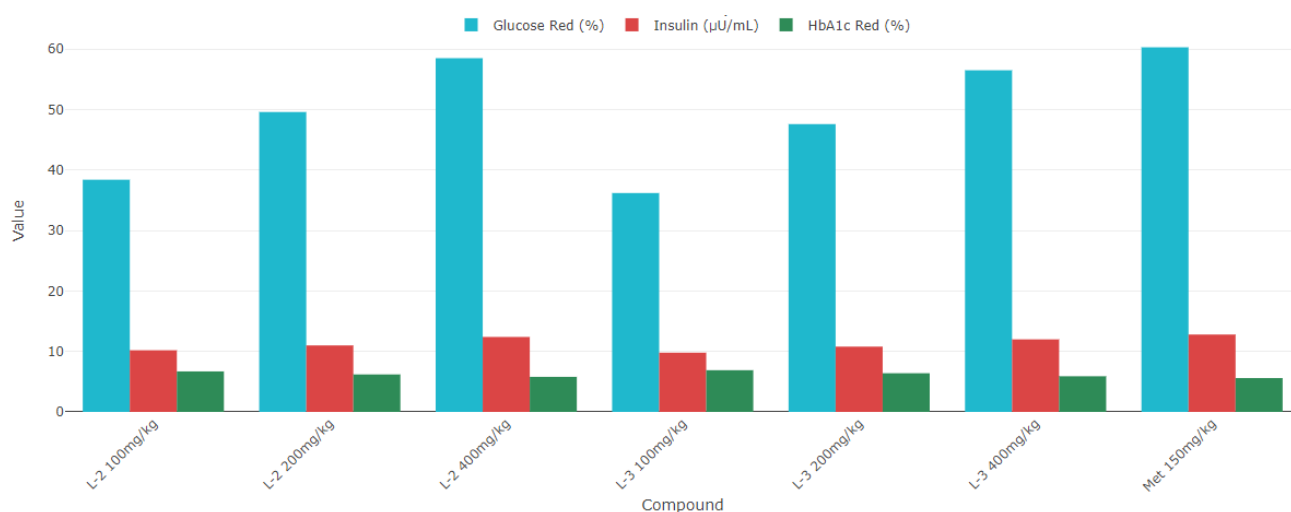


**Figure 6:** Dose-Response Analysis Comparison of antidiabetic effects by dose for compounds L-2 and L-3 versus metformin, evaluated through percentage reduction in glucose, changes in insulin ( $\mu\text{U/mL}$ ), and reduction in HbA1c (%), highlighting the dose-dependent efficacy.

<file:///C:/Users/hp/Desktop/ACADEMIC%20GROWTH/3rd%20month/metaanalysis/New%20folder/3...html>



## DISCUSSION

The comprehensive evaluation of the synthesized andrographolide derivatives revealed clear structure-activity relationships, providing insights for future drug development. The differential biological activities among the four derivatives can be attributed to specific structural modifications and their impact on molecular interactions with target enzymes.[14] The superior performance of L-2 and L-3 compared to L-1 and L-4 suggests that the nature of the nitrogen-containing substituent plays a critical role in modulating activity. L-2, featuring a piperidine ring, and L-3, containing a benzylamine moiety, demonstrated enhanced binding affinities and enzyme inhibitory activities. The cyclic piperidine structure in L-2 likely provides conformational rigidity, optimizing interactions with enzyme active sites, whereas the aromatic benzyl group in L-3 facilitates additional  $\pi$ - $\pi$  stacking interactions with aromatic residues in the binding pocket. In contrast, the linear aliphatic substituents in L-1 (allyl group) and L-4 (butyl chain) resulted in reduced binding affinities and weaker biological activity.[15-16] The increased conformational flexibility of these linear chains may hinder optimal positioning within the enzyme active site, leading to diminished inhibitory potency. Molecular docking analysis further revealed that L-2 and L-3 possess multiple hydrogen bond donors and acceptors, enabling extensive hydrogen bonding networks with active site residues, including tyrosine, lysine, and aspartate. These interactions stabilize the enzyme-inhibitor complex and compete with natural substrate binding, contributing to enhanced inhibitory activity.[17-18] The dual inhibition of  $\alpha$ -glucosidase and  $\alpha$ -amylase by L-2 and L-3 suggests a comprehensive mechanism for managing postprandial hyperglycemia.  $\alpha$ -Amylase initiates carbohydrate digestion by cleaving  $\alpha$ -1,4-glycosidic bonds in starch and glycogen, producing oligosaccharides and maltose.  $\alpha$ -Glucosidase, located in the brush border of small intestinal epithelial cells, subsequently converts these products to glucose for absorption.[19-20] By simultaneously inhibiting both enzymes, L-2 and L-3 effectively delay carbohydrate digestion and glucose absorption, reducing postprandial glucose excursions. This mechanism is particularly relevant for diabetes management, as postprandial hyperglycemia is strongly associated with diabetic complications and cardiovascular risk.[21-22] Docking studies indicated that hydrogen bonding with catalytic residues likely disrupts enzyme activity by directly blocking the active site or inducing conformational changes that reduce catalytic efficiency. Additional hydrophobic interactions observed with L-2 and L-3 contribute supplementary binding energy, enhancing inhibitor affinity and residence time within the active site. In vivo studies demonstrated that the derivatives exert multifaceted antidiabetic effects beyond enzyme inhibition. Significant improvements in serum insulin levels suggest potential enhancement of pancreatic  $\beta$ -cell function or insulin sensitivity.[23-24] These findings align with previous reports that andrographolide derivatives improve glucose uptake, insulin signaling, and pancreatic islet protection.

Reductions in HbA<sub>1c</sub> levels with L-2 and L-3 indicate effective long-term glycemic control. HbA<sub>1c</sub>, reflecting average blood glucose over 2–3 months, is a gold standard for assessing glycemic management. The ability of these derivatives to significantly reduce HbA<sub>1c</sub> highlights their potential to prevent chronic diabetic complications.[25] The observed dose-dependent effects further support the therapeutic potential of these compounds, with 400 mg/kg doses producing maximal benefits, while 100–200 mg/kg doses yielded proportionally reduced but statistically significant improvements. Compared to acarbose, a clinically approved  $\alpha$ -glucosidase inhibitor, L-2 and L-3 demonstrated comparable or superior in vitro enzyme inhibition.[26] Notably, acarbose is associated with gastrointestinal side effects such as flatulence, diarrhea, and abdominal discomfort due to bacterial fermentation of undigested carbohydrates. Preliminary safety assessments of the synthesized derivatives indicated no observable adverse effects, suggesting a potentially improved safety profile.[27] The in vivo efficacy of L-2 and L-3 also approached that of metformin, the first-line therapy for type 2 diabetes. This suggests these derivatives may serve as effective alternatives or adjuncts to existing therapies. While the current study demonstrates the antidiabetic potential of andrographolide derivatives, several limitations exist.[28] The in vivo evaluations were performed using an acute STZ-induced diabetes model over a short 28-day

period. Longer-term studies using chronic diabetes models are needed for comprehensive safety and efficacy data. Pharmacokinetic properties and bioavailability require detailed investigation. [29] Although structural modifications were designed to improve solubility and drug-likeness of andrographolide, formal pharmacokinetic studies are necessary to confirm enhanced drug-like properties. Future research should focus on several directions to strengthen the therapeutic potential of the studied compounds. [30] Comprehensive toxicological assessments are essential to establish long-term safety and tolerability. Mechanistic studies should be undertaken to elucidate the precise antidiabetic pathways, which will provide deeper insights into their biological activity and therapeutic relevance. Additionally, optimization of synthetic procedures is necessary to ensure scalable and cost-effective production for clinical and industrial applications. [31] It is also important to explore possible drug-drug interactions, as these may significantly influence efficacy and safety in patients receiving combination therapies. Furthermore, the development of advanced delivery systems, such as nanoformulations, could enhance bioavailability, reduce dosing frequency, and minimize adverse effects, thereby improving overall therapeutic outcomes. [32] The preclinical results highlight the potential for clinical translation of L-2 and L-3. Comparable efficacy to established antidiabetic agents, along with preliminary safety data, supports further development. The traditional use of *Andrographis paniculata* in diabetes management provides additional justification, potentially facilitating regulatory acceptance. Given the global diabetes epidemic and limitations of current therapies, these derivatives with their dual enzyme inhibition mechanism and additional antidiabetic effects represent promising candidates to address unmet clinical needs in diabetes management. [31-32]

## CONCLUSION

This research effectively synthesised and assessed new semisynthetic derivatives of andrographolide, revealing considerable antidiabetic efficacy. Four derivatives (L-1, L-2, L-3, and L-4) were synthesised by systematic chemical changes and thoroughly characterised using several analytical methods, including infrared spectroscopy, nuclear magnetic resonance, and mass spectrometry. The amalgamation of computational molecular docking, in vitro enzyme inhibition experiments, and in vivo effectiveness investigations yielded substantial proof of their medicinal promise. L-2 and L-3 were identified as the most promising derivatives, demonstrating enhanced  $\alpha$ -glucosidase and  $\alpha$ -amylase inhibitory actions with IC<sub>50</sub> values akin to the clinical standard acarbose. In vivo assessments validated notable antidiabetic outcomes, including considerable reductions in fasting blood glucose levels, enhancements in serum insulin, and advantageous decreases in HbA<sub>1c</sub>, akin to metformin therapy. Molecular docking investigations elucidated that the augmented activity of L-2 and L-3 is attributable to advantageous molecular interactions, including hydrogen bonding and hydrophobic contacts with enzyme active sites. The established structure-activity connections provide essential insights for the creation and enhancement of forthcoming derivatives. The dual enzyme inhibition demonstrated by these compounds offers potential benefits over single-target treatments by providing extensive control of postprandial hyperglycemia. Initial safety evaluations indicated no substantial negative effects, indicating potentially enhanced tolerance compared to current  $\alpha$ -glucosidase inhibitors. These findings provide a robust basis for the further development of andrographolide derivatives as innovative antidiabetic medicines. Subsequent research should concentrate on meticulous pharmacokinetic analysis, extensive toxicity assessments, refinement of the most promising derivatives, and eventual clinical trials to fully exploit their medicinal potential. This study shows the significance of natural product derivatisation in drug discovery, illustrating that deliberate chemical modifications can augment bioactivity while preserving safety, thus offering a promising pathway for the creation of effective and safer antidiabetic therapies that integrate traditional medicinal knowledge with contemporary pharmaceutical advancements.

## REFERENCES

1. Panossian A, Hovhannisyanyan A, Mamikonyan G, Abrahamyan H, Hambarzumyan E, Gabrielyan E, Goukasova G, Wikman G, Wagner H. Pharmacokinetic and oral bioavailability of andrographolide from *Andrographis paniculata* fixed combination Kan Jang in rats and human. *Phytomedicine*. 2000;7(5):351-364.
2. Akmal M, Wadhwa R, Kumar A. *Andrographis paniculata* extracts and andrographolide ameliorate oxidative stress and inflammation in carbon tetrachloride-induced liver injury in mice. *Biomed Pharmacother*. 2016;84:1608-1617.
3. Mohamed EA, Siddiqui MJ, Ang LF, Sadikun A, Chan SH, Tan SC, Asmawi MZ, Yam MF. Potent  $\alpha$ -glucosidase and  $\alpha$ -amylase inhibitory activities of standardized 50% ethanolic extracts and sinensetin from *Orthosiphon stamineus*. *BMC Complement Altern Med*. 2012;12:176.
4. Zhang S, Cheng H, Zhou L, Yu J, Wang C, Xie H, Huang L. Synthesis and biological evaluation of novel andrographolide derivatives as potential antitumor agents. *Bioorg Med Chem Lett*. 2021;43:128087.
5. Liu L, Yan Y, Zheng L, et al. *Andrographolide* and its analogues: Structure-activity relationships and biological activities. *Curr Med Chem*. 2020;27(39):6715-6739.
6. Menon V, Bhat S. Anticancer activity of andrographolide semisynthetic derivatives. *Nat Prod Commun*. 2010;5(5):717-720.
7. Akmal M, Wadhwa R. Alpha Glucosidase Inhibitors. In: StatPearls. StatPearls Publishing; 2024.
8. Kumar G, Singh S, Kumar A, et al. Chemical modification and its effect on biological activities of andrographolide. *Eur J Med Chem*. 2020;187:111958.
9. Messire G, Bauerová K, Rovenský J, et al. Synthetic Modifications of Andrographolide Targeting New Therapeutic Applications: A Review. *Molecules*. 2024;29(12):2842.
10. Kaya B, Menteşe E, Yılmaz F, et al. Synthesis,  $\alpha$ -Glucosidase,  $\alpha$ -Amylase, and Aldol Reductase Inhibitory Activity of Imidazo[1,2-a]pyridine-Based 1,3,4-Thiadiazole Derivatives. *ACS Omega*. 2024;9(41):42580-42588.
11. Shirisha K, Mastan M. *Andrographis paniculata* and its bioactive phytochemical constituents for oxidative damage: A systemic review. *Pharmacophore*. 2013;4(6):212-229.
12. Che C, Wang C, Zhang J, et al. Tricyclic Aza-Andrographolide Derivatives from Late-Stage Functionalization Show Potent Anti-HCoV Activity. *ACS Omega*. 2022;7(26):22429-22436.

13. Gajbhiye RL, Ganapathy A, Jaisankar P. A Review of  $\alpha$ -Glucosidase and  $\alpha$ -Amylase Inhibitors for Type 2 Diabetes Isolated from Some Important Indian Medicinal Plants. Remedy Publications LLC. 2016.
  14. Tung YT, Chua MT, Wang SY, Chang ST. Anti-inflammation activities of essential oil and its constituents from indigenous cinnamon (*Cinnamomum osmophloeum*) twigs. *Bioresour Technol.* 2008;99(9):3908-3913.
  15. Kumar G, Loganathan C, Mohan CG, et al. Site-Selective Synthesis of C-17 Ester Derivatives of Natural Andrographolide and Their Anticancer Activity. *ACS Omega.* 2023;8(5):4677-4691.
  16. Chelladurai GRM, Chinnachamy C. Alpha amylase and Alpha glucosidase inhibitory effects of aqueous stem extract of *Salacia oblonga* and its GC-MS analysis. *Braz J Pharm Sci.* 2018;54(1):e17151.
  17. Chauhan ES, Sharma K, Bist R. *Andrographis paniculata*: A Review of its Phytochemistry and Pharmacological Activities. *Research Journal of Pharmacy and Technology.* 2019;12(12):6030-6040.
  18. Ribeiro JRL, Lopéz-Vallejo F, Medina-Franco JL, et al. Nitrogen-containing andrographolide derivatives with multidrug resistance reversal effects in cancer cells. *RSC Med Chem.* 2024;15(4):1289-1303.
  19. Ullah H, Khan A, Baig MW, et al. A promising  $\alpha$ -glucosidase and  $\alpha$ -amylase inhibitors based on 7-azaindole: Synthesis, in vitro evaluation, kinetic study, pharmacophore modeling and molecular docking analysis. *Int J Biol Macromol.* 2024;254:127729.
  20. Abdullah S, Singh B, Sharma R, et al. A review on the molecular mechanisms and pharmacology of *Andrographis paniculata* (Burm.f.) Nees and andrographolide. *Phytomedicine Plus.* 2025;5(1):100454.
  21. Marzouk MA, Gamal-Eldeen AM, El-Hussieny EA, et al. Dual  $\alpha$ -amylase and  $\alpha$ -glucosidase inhibition by 1,2,4-triazole derivatives: Synthesis, enzyme kinetics and molecular docking insights for diabetes management. *Sci Rep.* 2025;15:1289.
  22. Hu J, Chen Y, Yang S, et al. The therapeutic potential of andrographolide in cancer treatment: From mechanisms to clinical applications. *Biomed Pharmacother.* 2024;171:116126.
23. Raksat, A. et al. Antibacterial and inhibitory activities against nitric oxide production of coumarinochromones and prenylated isoflavones from *Millettia extensa*. *J. Nat. Prod.* 82(8), 2343–2348 (2019).
  24. Jaidee, W. et al. Metabolite fingerprinting of *Piper nigrum* L. from different regions of Thailand by UHPLC-QTOF-MS approach and in vitro bioactivities. *Trends Sci.* 19(22), 1520–1532 (2022).
  25. Fitrasuah, S. I. et al. Analysis of chemical properties and antioxidant activity of Sambiloto (*Andrographis paniculata* Nees.) leaf tea formula as a functional drink in preventing coronavirus diseases and degenerative diseases. *J. Med. Sci.* 9, 196–201 (2021).
  26. Adeleye, O. A., Babalola, C. O., Femi-Oyewo, M. N. & Balogun, G. Y. Antimicrobial activity and stability of *Andrographis paniculata* cream containing Shea butter. *Nig J. Pharm. Res.* 15(1), 9–18 (2019).
  27. Limsiriwong, M., Sahamethapat, A. & Kanjanapruk, P. Development and validation of UPLC method for analysis of Andrographolide from *Andrographis paniculata* (Burm. f.) Nees. *J. Thai Trad Alt Med.* 17(2), 153–167 (2019).
  28. Pramanick, S. et al. Andropanolide and isoandrographolide, minor diterpenoids from *Andrographis paniculata*: Structure and X-ray crystallographic analysis. *J. Nat. Prod.* 69(3), 403–405 (2006).
  29. Xu, Y., Wei, H., Wang, J., Wang, W. & Gao, J. Synthesis of Andrographolide analogues and their neuroprotection and neurite outgrowth-promoting activities. *Bioorg. Med. Chem.* 27(11), 2209–2219 (2019).
  30. Kumar, G., Singh, D., Tali, J. A., Dheer, D. & Shankar, R. Andrographolide: Chemical modification and its effect on biological activities. *Bioorg. Chem.* 95, 103511 (2020).
  31. Rahman, M., Ayoob, I., Rehman, S., Bhat, K. A. & Ara, T. Microwave-assisted synthesis of Andrographolide analogues as potent  $\beta$ -glycosidase inhibitors. *SynOpen* 2(2), 200–206 (2018).
  32. Wen, Q., Jin, X., Lu, Y. & Chen, D. F. Anticomplement ent-labdane diterpenoids from the aerial parts of *Andrographis paniculata*. *Fitoterapia* 142, 104528 (2020).